Original Article | Thoracic Imaging

https://doi.org/10.3348/kjr.2018.19.3.526
pISSN 1229-6929 · eISSN 2005-8330
Korean J Radiol 2018;19(3):526-533

Korean Journal of Radiology
KJR

The Potential Role of Grid-Like Software in Bedside Chest Radiography in Improving Image Quality and Dose Reduction: An Observer Preference Study

Su Yeon Ahn, MD[1, 2], Kum Ju Chae, MD[1, 3], Jin Mo Goo, MD, PhD[1, 4]

[1]Department of Radiology, Seoul National University College of Medicine, and Institute of Radiation Medicine, Seoul National University Medical Research Center, Seoul 03080, Korea; [2]Department of Radiology, Konkuk University Medical Center, Konkuk University School of Medicine, Seoul 05030, Korea; [3]Department of Radiology, Institute of Medical Science, Research Institute of Clinical Medicine, Chonbuk National University Medical School and Hospital, Jeonju 54907, Korea; [4]Cancer Research Institute, Seoul National University College of Medicine, Seoul 03080, Korea

Objective: To compare the observer preference of image quality and radiation dose between non-grid, grid-like, and grid images.
Materials and Methods: Each of the 38 patients underwent bedside chest radiography with and without a grid. A grid-like image was generated from a non-grid image using SimGrid software (Samsung Electronics Co. Ltd.) employing deep-learning-based scatter correction technology. Two readers recorded the preference for 10 anatomic landmarks and the overall appearance on a five-point scale for a pair of non-grid and grid-like images, and a pair of grid-like and grid images, respectively, which were randomly presented. The dose area product (DAP) was also recorded. Wilcoxon's rank sum test was used to assess the significance of preference.
Results: Both readers preferred grid-like images to non-grid images significantly ($p < 0.001$); with a significant difference in terms of the preference for grid images to grid-like images ($p = 0.317$, 0.034, respectively). In terms of anatomic landmarks, both readers preferred grid-like images to non-grid images ($p < 0.05$). No significant differences existed between grid-like and grid images except for the preference for grid images in proximal airways by two readers, and in retrocardiac lung and thoracic spine by one reader. The median DAP were 1.48 (range, 1.37–2.17) dGy*cm^2 in grid images and 1.22 (range, 1.11–1.78) dGy*cm^2 in grid-like images with a significant difference ($p < 0.001$).
Conclusion: The SimGrid software significantly improved the image quality of non-grid images to a level comparable to that of grid images with a relatively lower level of radiation exposure.
Keywords: *Bedside chest radiography; Scatter correction; Software; Image quality; Dose reduction; Grid*

INTRODUCTION

The use of bedside chest radiography has been increasing continually with the increase in aging population and the need for care of critically ill patients. Bedside chest radiography provides information that may not be obtained clinically such as malposition of invasive devices or detection of cardiopulmonary deterioration, which is crucial for disease management (1, 2). However, bedside examination has a major limitations involving

Received August 26, 2017; accepted after revision November 23, 2017.
This study was supported in part by grant from the Samsung Electronics Research Fund and in part by a grant of the Korea Health Technology R&D Project through the Korea Health Industry Development Institute (KHIDI), funded by the Ministry of Health & Welfare, Republic of Korea (grant number : HI15C1532).
Corresponding author: Jin Mo Goo, MD, PhD, Department of Radiology, Seoul National University College of Medicine, and Institute of Radiation Medicine, Seoul National University Medical Research Center, 101 Daehak-ro, Jongno-gu, Seoul 03080, Korea.
• Tel: (822) 2072-2624 • Fax: (822) 743-7418 • E-mail: jmgoo@plaza.snu.ac.kr

Korean Journal of Radiology
KJR

image degradation by scattered radiation (3). Although anti-scatter grid improves the contrast by reducing the scattered radiation, many hospitals do not use grid in bedside examinations for various reasons. Using a grid in a bedside investigation is challenging due to the risk of misalignment and grid cutoff, which reduces diagnostic information. Additional radiation is required for repeat examinations if necessary. Furthermore, grid transportation and positioning is an additional technological burden, and grid usage typically entails a higher radiation dose. Eventual damage requires grid installation and replacement, and related costs. To overcome these limitations, researchers developed software that provides scatter correction without the physical use of a grid (4-7). The technology enables estimation of the scatter signal and calculation of the grid effect. The recently introduced 'SimGrid' scatter correction software (Samsung Electronics Co. Ltd., Suwon, Korea) allows the estimation of the distribution and degree of scatter radiation using raw image data directly with pre-trained Convolutional Neural Networks. These networks have been trained and optimized using tens of thousands of anthropomorphic phantoms and clinical images. Thus, it is robust under varying conditions of exposure, patient status, and positional changes. The estimated scatter image is subtracted from the raw image to produce a de-scattered image. Subsequently, the de-scattered raw image is processed by the post-processing software of the digital radiography system. Although the value of scatter correction in terms of physical properties using a phantom has been reported (6, 7), no test of observer preference has been performed to facilitate clinical application of this software.

Therefore, the purpose of our study was to compare the observer preference of image quality and radiation dose between non-grid and grid-like images generated by scatter correction software, and between grid-like and grid images.

MATERIALS AND METHODS

Support and Funding

This study was financially and technically supported by Samsung Electronics Corporation. However, the company had no control over any data or information submitted for publication or over any data or information included in this study.

Patients

This prospective study was approved by the Institutional Review Board of our institution and written consent was obtained from all participating patients. Patients who presented for scheduled routine follow-up for chest radiography at our institution were considered for inclusion. Patients who were unable to provide written informed consent or who were pregnant or expecting pregnancy in the near future were excluded. Patients who consented to chest radiography with and without grid were enrolled between January 17 2017 and February 17 2017. Our study population included a total of 38 patients (male-to-female ratio, 25:13; median age, 57 years; age range, 24–78 years).

Image Acquisition

Participants underwent chest radiography with the anteroposterior projection. All the investigations were performed with a mobile X-ray system GM85 (Samsung Electronics Co. Ltd.) using a 345 x 426 mm detector. Grid images were acquired using a 6:1 grid with 85 L/cm density and a focal distance of 130 cm. Three image sets were obtained for each patient. An image was acquired with grid (grid image), and another image without grid (non-grid image) immediately to minimize the positional change. The other image was obtained via post-processing with SimGrid software using non-grid image (grid-like image). Exposure parameters were as follows: source-to-object distance, 100 cm; focal spot size, 1.2 mm; tube voltage, 80–90 kVp; tube current 230–240 mA; and exposure time, 5 ms.

Radiation Dose Estimations

All the exposure factors were recorded. The dose area product (DAP [$cGy \cdot cm^2$]) was calculated using the S-DAP algorithm (Samsung Electronics Co. Ltd.), which enables calculation of the area dose under conditions such as tube voltage, tube current, the presence or absence of additional filters, filter thickness, and collimator size, instead of using DAP meter.

Image Evaluation

Two radiologists (Reader 1 and 2, with 26 and 5 years of experience in chest radiology, respectively) independently compared the paired images of (a) non-grid and grid-like images followed by (b) grid-like and grid images randomly. The readers were blinded to patient and clinical demographics. All the data were stored in Digital Imaging and Communications in Medicine format. The window width and window level of the images were automatically optimized by the customized program. Readers were

allowed to adjust the brightness and contrast of the images. The anatomic landmarks used for image evaluation were similar to those of previous studies dealing with chest radiography (8). The 10 anatomic landmarks included the unobscured lung, hilum, minor fissure, retrocardiac lung, subdiaphragmatic lung, azygoesophageal recess, heart border, rib, proximal airway, and thoracic spines. The overall image quality was also evaluated. Images were graded using a five-point scale from one to five (1, strongly preferred A; 2, somewhat preferred A; 3, no preference; 4, somewhat preferred B; 5, strongly preferred B [A = initial image, B = second image]). The score was rearranged to A as non-grid images and B as grid-like images in test 1, and to A as grid images and B as grid-like images in test 2 since each pair of images was randomly arranged.

Sample Size Calculation

Sample size calculation was performed with the StatsDirect Statistical Software Version 3.1.11 (StatsDirect Ltd, Altrincham, UK), which revealed a sample size of 34 matched pairs of subjects to yield a power of 0.8, α = 0.05 for the detection of a mean difference of 11 with an estimated standard deviation of 22. The mean difference was determined based on the range rule for standard

Table 1. Comparison of Non-Grid Images with Grid-Like Images for 11 Anatomic Regions

Anatomic Regions	1	2	3	4	5	Mean	*P*
Unobscured lung							
Reader 1	0	0	0	28	10	4.3	< 0.001
Reader 2	0	0	1	19	18	4.4	< 0.001
Hilum							
Reader 1	0	0	14	22	2	3.7	< 0.001
Reader 2	0	0	4	26	8	4.1	< 0.001
Minor fissure							
Reader 1	0	0	19	15	4	3.6	< 0.001
Reader 2	0	0	30	8	0	3.2	0.005
Rib							
Reader 1	0	0	6	28	4	3.9	< 0.001
Reader 2	0	0	0	32	6	4.2	< 0.001
Heart border							
Reader 1	0	0	24	14	0	3.4	< 0.001
Reader 2	0	0	5	32	1	3.9	< 0.001
Retrocardiac lung							
Reader 1	0	0	5	25	8	4.1	< 0.001
Reader 2	0	0	5	28	5	4.0	< 0.001
Subdiaphragmatic lung							
Reader 1	0	0	11	17	10	4.0	< 0.001
Reader 2	0	0	18	18	2	3.6	< 0.001
Azygoesophageal recess							
Reader 1	0	0	21	12	5	3.6	< 0.001
Reader 2	0	0	27	5	6	3.4	0.003
Proximal airway							
Reader 1	0	0	11	19	8	3.9	< 0.001
Reader 2	0	0	10	28	0	3.7	< 0.001
Thoracic spine							
Reader 1	0	0	5	14	19	4.4	< 0.001
Reader 2	0	0	0	33	5	4.1	< 0.001
Overall appearance							
Reader 1	0	0	4	28	6	4.1	< 0.001
Reader 2	0	0	0	33	5	4.1	< 0.001

1 = strongly preferred non-grid images, 2 = somewhat preferred non-grid images, 3 = no preference, 4 = somewhat preferred grid-like images, 5 = strongly preferred grid-like images

Korean Journal of Radiology
KJR

deviation. Considering a dropout rate of 10%, a sample size of 38 was required.

Statistical Analysis

Wilcoxon's signed rank test was used to assess the significance of differences between ratings. An analysis of each reviewer was performed. As normal distribution of DAP was rejected by the Kolmogorov-Smirnov test, Wilcoxon's signed rank test was used to compare the radiation dose. All the statistical tests were two-sided with a significance level of 0.05. The statistical analysis was performed using SPSS (SPSS version 23.0; IBM Corp., Armonk, NY, USA).

RESULTS

Preference Study

Non-Grid vs. Grid-Like Images

The composite data for both readers in each anatomic region are summarized in Table 1.

The interpreters strongly preferred grid-like images to non-grid images for all anatomic landmarks and overall

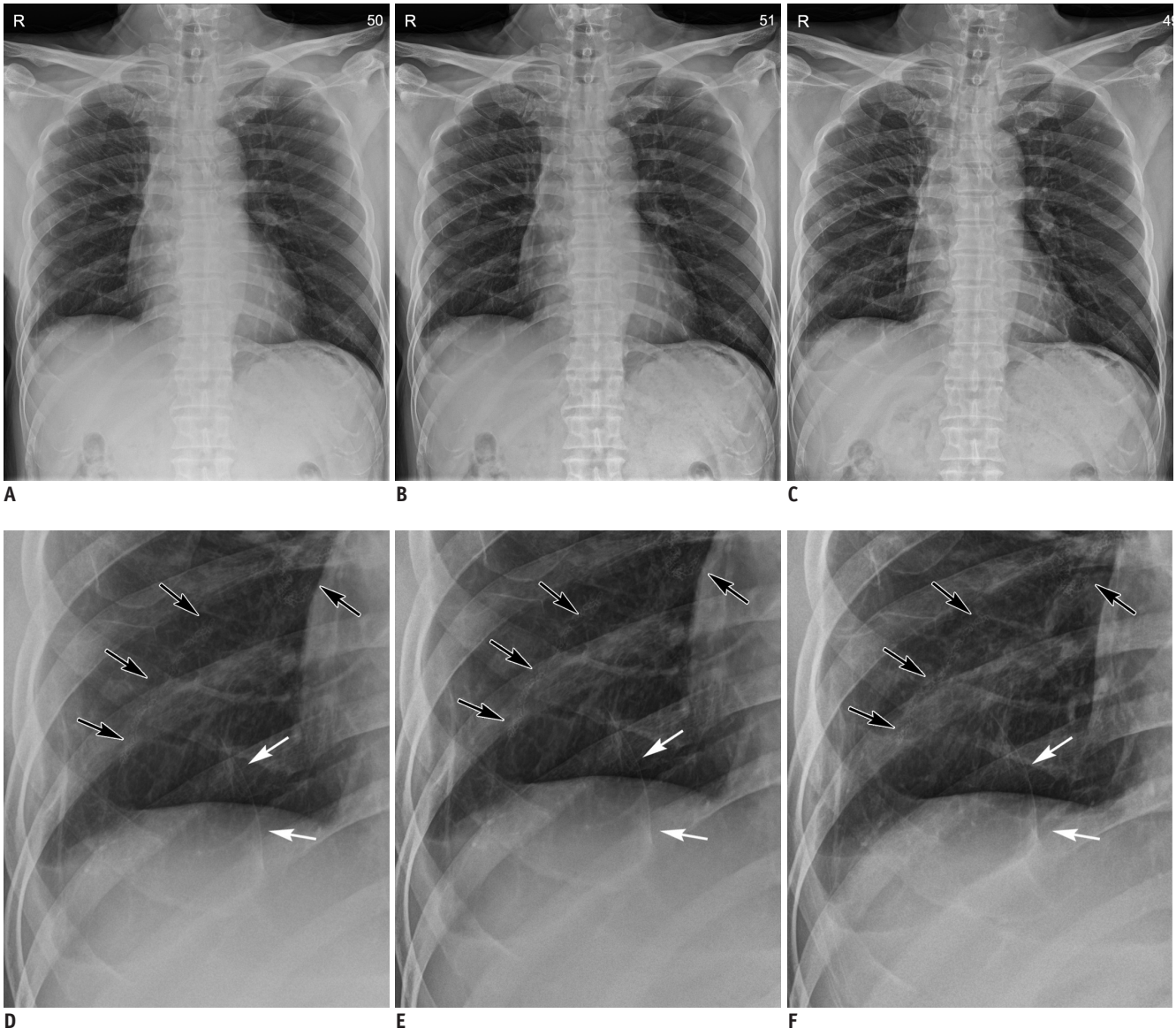

Fig. 1. Comparison of (A, D) non-grid, (B, E) grid-like, and (C, F) grid images.
A-C. Chest radiography of 57-year-old male patient who underwent multiple-wedge resection in both lungs for metastasis associated with undifferentiated pleomorphic sarcoma. Note superior image contrast of grid-like image to non-grid image, and similarity in contrast appearance between grid-like and grid images. **D-F.** Magnified non-grid, grid-like and grid images: surgical materials (black arrows) and multiple linear opacities (white arrows) are clearly demonstrated in grid-like image, as well as grid image.

image quality ($p < 0.05$) (Figs. 1-3). The most preferred region included unobscured lung (mean, 4.4), followed by thoracic spine (mean, 4.3), overall appearance (mean, 4.1), rib (mean, 4.1), retrocardiac lung (mean, 4.1), hilum (mean, 3.9), subdiaphragmatic lung (mean, 3.8), proximal airway (mean, 3.8) and heart border (mean, 3.7) and azygoesophageal recess (mean, 3.5). The minor fissure was the least, but also preferred region (mean, 3.4).

Grid vs. Grid-Like Images

Neither reader indicated preference for any of the seven regions (unobscured lung, hilum, minor fissure, rib, heart border, subdiaphragmatic lung, azygoesophageal recess) (Fig. 1). Grid images were preferred to grid-like images in proximal airways by both readers ($p = 0.002$ and 0.001, respectively) (Fig. 2). For retrocardiac lung and thoracic spine, Reader 1 preferred grid-images to grid-like images ($p < 0.001$ and 0.014, respectively) (Fig. 3). Reader 1 rated equally for overall appearance ($p = 0.317$), while Reader 2 preferred grid images ($p = 0.034$). The composite data for both readers in each anatomic region are summarized in Table 2.

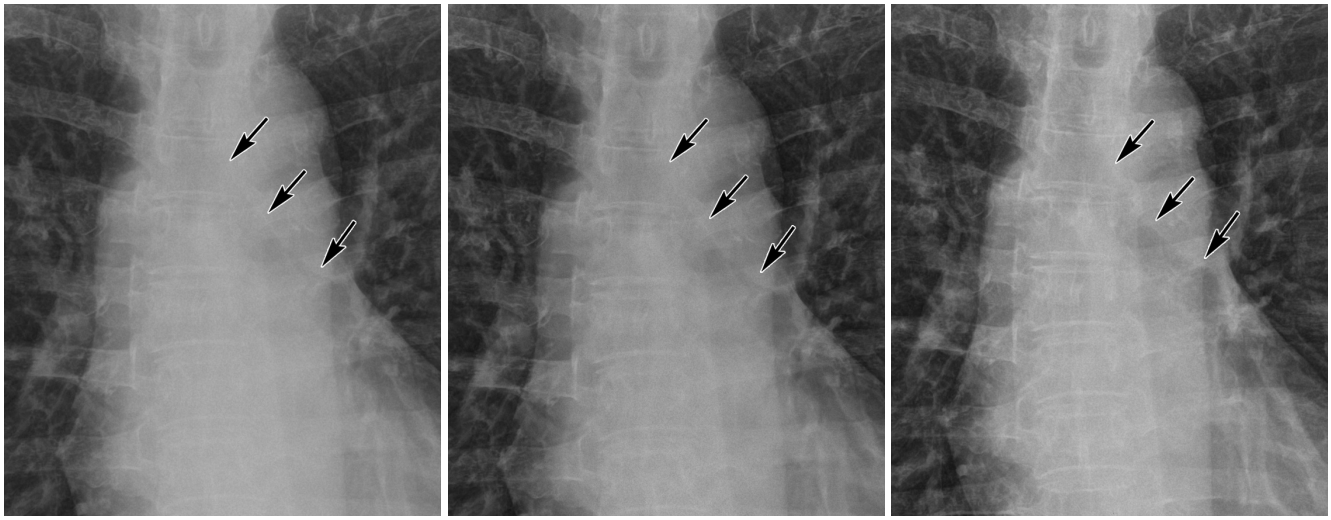

Fig. 2. Magnified anteroposterior chest radiographs of 59-year-old female with ovarian cancer.
Compared with **(A)** non-grid image, delineation of trachea and left main bronchus (arrows) is improved in **(B)** grid-like image, as well as **(C)** grid image.

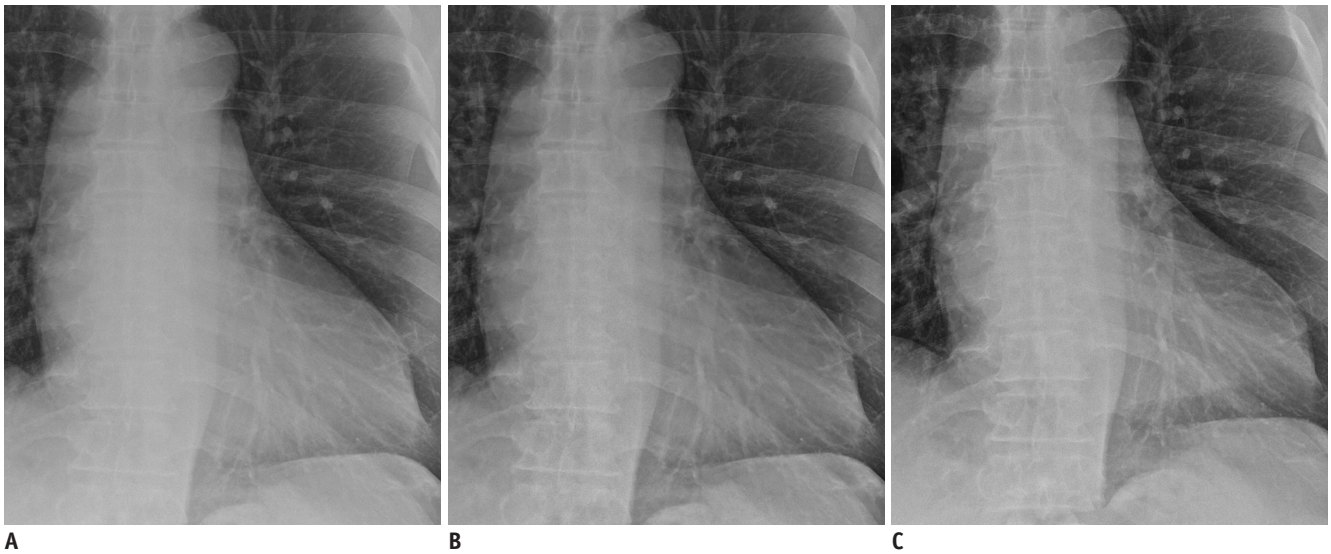

Fig. 3. Magnified anteroposterior chest radiographs of 63-year-old male with hepatocellular carcinoma.
Compared with **(A)** non-grid image, delineation of vascular shadows in retrocardiac area is improved in **(B)** grid-like image, as well as **(C)** grid image.

Korean Journal of Radiology
KJR

Table 2. Comparison of Grid Images with Grid-Like Images for 11 Anatomic Region

Anatomic Regions	1	2	3	4	5	Mean	*P*
Unobscured lung							
Reader 1	0	1	37	0	0	3.0	0.317
Reader 2	0	7	28	3	0	2.9	0.206
Hilum							
Reader 1	0	0	38	0	0	3.0	1.000
Reader 2	0	0	37	1	0	3.0	0.317
Minor fissure							
Reader 1	0	8	26	4	0	2.9	0.248
Reader 2	0	2	36	0	0	2.9	0.157
Rib							
Reader 1	0	1	37	0	0	3.0	0.317
Reader 2	0	0	38	0	0	3.0	1.000
Heart border							
Reader 1	0	1	37	0	0	3.0	0.317
Reader 2	0	0	38	0	0	3.0	1.000
Retrocardiac lung							
Reader 1	0	19	18	1	0	2.5	< 0.001
Reader 2	1	2	35	0	0	2.9	0.102
Subdiaphragmatic lung							
Reader 1	0	15	17	6	0	2.8	0.050
Reader 2	1	3	34	0	0	2.9	0.059
Azygoesophageal recess							
Reader 1	0	1	37	0	0	3.0	0.317
Reader 2	2	2	33	1	0	2.9	0.129
Proximal airway							
Reader 1	0	10	28	0	0	2.7	0.002
Reader 2	0	11	27	0	0	2.7	0.001
Thoracic spine							
Reader 1	0	6	32	0	0	2.8	0.014
Reader 2	0	1	37	0	0	3.0	0.317
Overall appearance							
Reader 1	0	1	37	0	0	3.0	0.317
Reader 2	0	7	30	1	0	2.8	0.034

Radiation Dose

The median DAP were 1.48 (range, 1.37–2.17) dGy*cm^2 in grid images and 1.22 (range, 1.11–1.78) dGy*cm^2 in non-grid and grid-like images. Wilcoxon's signed rank test demonstrated a significant difference between grid and grid-like images ($p < 0.001$).

DISCUSSION

Grid-like images were highly preferred to non-grid images in all the 10 anatomic landmarks and overall appearance. It is noteworthy the quality of grid-like images was equivalent to that of grid images.

The highest scoring regions included unobscured lungs, followed by thoracic spines and retrocardiac lungs using SimGrid compared with non-grid images. Contrast improvement using an anti-scatter grid is known to be associated with local scatter fraction. The scatter fraction is the ratio of the intensity of scatter radiation to that of total (scattered plus unscattered) radiation recorded on the image. Scatter fraction values were higher in the mediastinum and retrocardiac regions than the lungs (9), which explains our findings indicating that retrocardiac lungs and thoracic spines were among the most preferred regions. A greater scatter occurring in these regions suggested higher chances of restoration of the contrast using scatter correction software. Interestingly, unobscured lungs were the most preferred areas despite a relatively

low scatter fraction. Unobscured lungs occupy the largest area in a chest radiograph and, under high natural contrast, readers may recognize significant improvements in this region.

Scatter radiation has been reduced traditionally by modifying the image acquisition process using hardware. The introduction of a grid for mobile applications improved the image quality (10-13). However, only 12% of radiologists and technologists used anti-scatter grids for bedside chest radiography according to Wandtke's survey (3). The most frequent suggestion to improve the image quality of bedside chest radiography was to use grids regularly and consistently. Laser-alignment and automatic grid alignment systems were developed to improve the control of grid positioning (14, 15). The recently developed bedside digital radiography is equipped to display the current detector angle on the screen for proper alignment. However, despite such developments facilitating tube detector alignment, the grid has yet to be used in bedside examinations widely. Precise positioning and alignment are still difficult because patients are still the focus of technologists rather than equipment screen when determining the grid position. Further, cumbersome workflow parameters include grid attachment and detachment, as well as disinfection after usage. Concerns related to additional radiation dosage when using grid or performing repeated examinations due to grid misalignment also need to be addressed.

With the introduction of digital imaging, an alternate approach has been developed to compensate for image degradation through digital image processing. Recently, several vendors have developed new software that estimates the scattered radiation and provides scatter correction without the usage of grids (4, 5, 7, 16). The technology saved 15 seconds to 34 seconds per examination on average compared with grid-based workflow (5, 17), resulting in workflow improvement by 28% (17). Mentrup et al. (6) conducted experiments investigating the performance of a software-based scatter correction and demonstrated contrast improvement by software consistent with the results obtained using the grid quantitatively. It is in accordance with our results showing that the quality of grid-like images is comparable to that of grid images while reducing radiation dose by 18.7%. The findings suggest that SimGrid software facilitates reduction in dose as well as workload.

There are several limitations in this study. First, non-grid images were easily identified due to conspicuous differences even though they were blinded, which could lead to a bias. However, it was not easy to differentiate grid-like from grid images. Second, the study population is composed of patients who visited the outpatient clinic, suggesting differences under a clinical setting. Most patients in bedside settings do not cooperate with chest examination such as positioning and breath-holding. However, these conditions pose a bigger challenge in grid images than in grid-like images. Third, as this is an observer preference study, it is unknown whether a better preference can be interpreted as better observer performance. Further studies investigating the impact of SimGrid software on diagnostic performance are needed. Most importantly, under optimal conditions excluding bedside radiography, grid-based radiography is still superior to non-grid radiography. Therefore, the results do not indicate if this application can replace radiography using a grid under all circumstances.

In conclusion, SimGrid software improved the image quality of non-grid images significantly to a level comparable to that of grid images under a relatively lower level of radiation exposure.

REFERENCES

1. Rubinowitz AN, Siegel MD, Tocino I. Thoracic imaging in the ICU. *Crit Care Clin* 2007;23:539-573
2. Eisenhuber E, Schaefer-Prokop CM, Prosch H, Schima W. Bedside chest radiography. *Respir Care* 2012;57:427-443
3. Wandtke JC. Bedside chest radiography. *Radiology* 1994;190:1-10
4. Kawamura T, Naito S, Okano K, Yamada M. Improvement in image quality and workflow of x-ray examinations using a new image processing method, "Virtual Grid Technology". Web site. http://www.fujifilm.com/about/research/report/060/pdf/index/ff_rd060_004_en.pdf. Published 2015. Accessed July 13, 2017
5. Mentrup D, Specht S, Spieckermann J, Zorba G. Grid-less imaging with SkyFlow: time savings and workflow improvements. Web site. https://www.usa.philips.com/b-dam/b2bhc/us/topics/radiology-patience-experience/SkyFlow-whitepaper-452299111471_LR.PDF. Published June 2015. Accessed July 13, 2017
6. Mentrup D, Jockel S, Menser B, Neitzel U. Iterative scatter correction for grid-less bedside chest radiography: performance for a chest phantom. *Radiat Prot Dosimetry* 2016;169:308-312
7. Renger B, Brieskorn C, Toth V, Mentrup D, Jockel S, Lohöfer F, et al. Evaluation of dose reduction potentials of a novel scatter correction software for bedside chest X-ray imaging. *Radiat Prot Dosimetry* 2016;169:60-67
8. Goo JM, Im JG, Kim JH, Seo JB, Kim TS, Shine SJ, et al.

Digital chest radiography with a selenium-based flat-panel detector versus a storage phosphor system: comparison of soft-copy images. *AJR Am J Roentgenol* 2000;175:1013-1018
9. Floyd CE Jr, Baker JA, Lo JY, Ravin CE. Measurement of scatter fractions in clinical bedside radiography. *Radiology* 1992;183:857-861
10. Anderson DW. Introduction of grids to mobile ICU radiography in a teaching hospital. *Br J Radiol* 2006;79:315-318
11. Moore CS, Wood TJ, Avery G, Balcam S, Needler L, Smith A, et al. Investigating the use of an antiscatter grid in chest radiography for average adults with a computed radiography imaging system. *Br J Radiol* 2015;88:20140613
12. Scott AW, Gauntt DM, Yester MV, Barnes GT. High-ratio grid considerations in mobile chest radiography. *Med Phys* 2012;39:3142-3153
13. Uffmann M, Schaefer-Prokop C. Digital radiography: the balance between image quality and required radiation dose. *Eur J Radiol* 2009;72:202-208
14. Gauntt DM, Barnes GT. An automatic and accurate x-ray tube focal spot/grid alignment system for mobile radiography: system description and alignment accuracy. *Med Phys* 2010;37:6402-6410
15. MacMahon H, Yasillo NJ, Carlin M. Laser alignment system for high-quality portable radiography. *Radiographics* 1992;12:111-120
16. Chae KJ, Goo JM, Ahn SY, Yoo JY, Yoon SH. Application of deconvolution algorithm of point spread function in improving image quality: an observer preference study on chest radiography. *Korean J Radiol* 2018;19:147-152
17. Lee K, Lee K, Lee S, Kim H. Workflow improvement with Samsung SimGrid SW. Web site. https://www.samsungmedicalsolution.com/en/common/whitePaper. Published February 22, 2016. Accessed July 13, 2017